Cellular Physiology and Biochemistry

Cell Physiol Biochem 2018;51:961-978
DOI: 10.1159/000495399
Published online: 22 November 2018
Accepted: 14 November 2018

© 2018 The Author(s)
Published by S. Karger AG, Basel
www.karger.com/cpb

Karger Open access

This article is licensed under the Creative Commons Attribution-NonCommercial-NoDerivatives 4.0 International License (CC BY-NC-ND) (http://www.karger.com/Services/OpenAccessLicense). Usage and distribution for commercial purposes as well as any distribution of modified material requires written permission.

Original Paper

Interferon Consensus Sequence-Binding Protein 8, a Tumor Suppressor, Suppresses Tumor Growth and Invasion of Non-Small Cell Lung Cancer by Interacting with the Wnt/β-Catenin Pathway

Lin Ye[a,b] Tingxiu Xiang[a] Jing Zhu[c] Dairong Li[d] Qin Shao[e] Weiyan Peng[a] Jun Tang[a] Lili Li[f] Guosheng Ren[a]

[a]Chongqing Key Laboratory of Molecular Oncology and Epigenetics, the First Affiliated Hospital of Chongqing Medical University, Chongqing, [b]Department of cardiothoracic surgery, the First Affiliated Hospital of Chongqing Medical University, Chongqing, [c]Department of Oncology, the First Affiliated Hospital of Chongqing Medical University, Chongqing, [d]Cytology Lab, Department of Respiration, the First Affiliated Hospital of Chongqing Medical University, Chongqing, [e]Department of Breast Disease Treatment Center, Chongqing University Cancer Hospital& Chongqing Cancer Institute, Chongqing, [f]Cancer Epigenetics Laboratory, Department of Clinical Oncology, State Key Laboratory of Oncology in South China, Sir YK Pao Center for Cancer and Li Ka Shing Institute of Health Sciences, the Chinese University of Hong Kong, Hong Kong, China

Key Words
IRF8 • NSCLC • Tumor suppressor • CpG methylation • TCF/LEF • Wnt/β-catenin

Abstract
Background/Aims: Interferon consensus sequence-binding protein 8 (IRF8) belongs to a family of interferon (IFN) regulatory factors that modulates various important physiological processes including carcinogenesis. As reported by others and our group, IRF8 expression is silenced by DNA methylation in both human solid tumors and hematological malignancies. However, the role of IRF8 in lung carcinoma remains elusive. In this study, we determined IRF8 epigenetic regulation, biological functions, and the signaling pathway involved in non-small cell lung cancer (NSCLC). ***Methods:*** IRF8 expression were determined by Q- PCR. MSP and A+T determined promotor methylation. MTS, clonogenic, Transwell assay, Flow cytometry, three-dimensional culture and AO/EB stain verified cell function. In vivo tumorigenesis examed the *in vivo* effects. By Chip-QPCR, RT-PCR, Western blot and Immunofluorescence staining, the mechanisms were studied. ***Results:*** IRF8 was significantly downregulated in lung tumor tissues compared with adjacent non-cancerous tissues. Furthermore, methylation-specific PCR analyses revealed that *IRF8* methylation in NSCLC was a common event, and

Guosheng Ren
and Tingxiu Xiang

Chongqing Key Laboratory of Molecular Oncology and Epigenetics, the First Affiliated Hospital of Chongqing Medical University, Chongqing (China)
Tel. (86) 23-89012558, Fax (86) 23-89012558, E-Mail rgs726@126.com; larissaxiang@163.com

demethylation reagent treatment proved that downregulation of *IRF8* was due to its promoter CpG hypermethylation. Clinical data showed that the *IRF8* methylation was associated with tumor stage, lymph node metastasis status, patient outcome, and tumor histology. Exogenous expression of IRF8 in the silenced or downregulated lung cancer cell lines A549 and H1299 at least partially restored the sensitivity of lung cancer cells to apoptosis, and arrested cells at the G0/G1 phase. Cell viability, clonogenicity, and cell migration and invasive abilities were strongly inhibited by restored expression of IRF8. A three-dimensional culture system demonstrated that IRF8 changed the cells to a more spherical phenotype. Moreover, ectopic expression of IRF8 enhanced NSCLC chemosensitivity to cisplatin. Furthermore, as verified by Chip-qPCR, immunofluorescence staining, and western blotting, IRF8 bound to the T-cell factor/lymphoid enhancer factor (TCF /LEF) promoter, thus repressing β-catenin nuclear translocation and its activation. IRF8 significantly disrupted the effects of Wnt agonist, bml284, further suggesting its involvement in the Wnt/β-catenin pathway. ***Conclusion:*** IRF8 acted as a tumor suppressor gene through the transcriptional repression of β-catenin-TCF/LEF in NSCLC. IRF8 methylation may serve as a potential biomarker in NSCLC prognosis.

© 2018 The Author(s)
Published by S. Karger AG, Basel

Introduction

Lung cancer is a common cancer worldwide, and is the leading cause of cancer mortality [1-3], most of which is from non-small cell lung cancer (NSCLC). The 5-year survival rate for lung cancer is only 17% [4]; therefore, identifying biomarkers for early diagnosis of lung cancer is crucial. There are accumulating evidences that aberrant DNA methylation is an important step in lung cancer. Recognition of tumor suppressor genes silenced or inhibited by DNA methylation could provide a better understanding of lung carcinogenesis, and may help to identify natural biomarkers for diagnosis and prognosis of lung cancer [5].

In a previous study by our group, we reported *IRF8* as the only downregulated gene within the 16q24 chromosome [6]. It was frequently epigenetically inactivated in nasopharyngeal carcinoma, esophageal cancer, breast cancer, cervical cancer, and especially in lung carcinoma [6]. Methylation of the *IRF8* promoter abolishes its response to interferon gamma (IFN-γ). Although IRF8 was reported to regulate apoptosis and evidence suggested it may possess some kind of function in lung cancer development, its role and mechanisms in lung cancer remain unknown [6].

The canonical Wnt /β-catenin pathway is a well-known oncogenic pathway in cancer development. Although its role is mainly in colon and breast cancer, emerging evidence suggests that it is also closely associated with lung cancer initiation and prognosis [7-9]. In the Wnt/β-catenin canonical pathway, the nuclear translocation of β-catenin from the cytoplasm to the nucleus is the key step to mediate the transcription of target genes. β-catenin first binds to the HMG-type transcription factor lymphoid enhancer factor-1 (LEF-1), resulting in the nuclear translocation of the β-catenin-LEF /TCF complex. The complex then binds to the promoter region of the E-cadherin gene and then activates the downstream targets [10, 11].

IRF8 functions as an anti-oncoprotein that inhibits the expression of a Wnt target gene, *myc*, negatively controls anti-apoptotic genes, such as *bcl2*, *bcl2l1* (*bcl-xl*), or *Ptpn13* (Fas-associated phosphatase-1), and enhances the expression of proapoptotic genes, such as caspase-3 expression [12, 13]. Recent studies have also shown that activation of β-catenin resulted in upregulation of IRF8, and IRF8, in turn, repressed the oncogenic function of β-catenin [14].

In this study, we demonstrated the epigenetic regulation of *IRF8*, its anti-cancer function, the interaction with the Wnt /β-catenin pathway in NSCLC, and most importantly, we addressed how IRF8 represses the oncogenic function of β-catenin.

Materials and Methods

Cell lines and tumor samples

NSCLC cell lines (A549, H1299) were used. These cell lines were from Professor Tao Qian, Chinese University of Hong Kong, Hong Kong, China. All cell lines were cultured in RPMI 1640 media (Gibco-BRL, Karlsruhe, Germany) with 10% fetal bovine serum (FBS; PAA Laboratories, Linz, Austria), at 37°C in a humidified atmosphere containing 5% CO_2 [15, 16]. Fresh NSCLC tissues and tumor adjacent tissues were obtained from patients who underwent lobectomy at the Department of Cardiothoracic Surgery, the First Affiliated Hospital of Chongqing Medical University.

Table 1. List of primers used in this study

Primer	Sequence(5'-3')	Product size
IRF8F	TCCGGATCCCTTGGAAACAC	240bp
IRF8R	CCTCAGGAACAATTCGGTAA	
GAPDHF	GGAGTCAACGGATTTGGT	206bp
GAPDHR	GTGATGGGATTTCCATTGAT	
β-actinF	TCCTGTGGCATCCACGAAACT	315bp
β-actinR	GAAGCATTTGCGGTGGACGAT	
LEF1F	TCCTTGGTGAACGAGTCTGA	247bp
LEF1R	TTCTCGGGATGGGTGGAGAA	
LEF1chipF1	TTCTCAGTCCCAGATTCCCGC	
LEF1chipR1	TCCTCTGCCAGTCTCTCCCC	160bp
LEF1chipF2	GGGAGAGACTGGCAGAGGA	
LEF1chipR2	CTTGGCGAGAGAAGGAAGGAC	168bp
LEF1chipF3	AACTCAGAGAGGGAGGAAGGG	
LEF1chipR3	CAAAAAGACCGAAGGCGAAAC	272bp
TCF4F	TGCATCACCAACAGCGAATG	
TCF4R	TGAGCCAGTAAAATGTCCACT	143bp

Clinical and pathological parameters of all the participants were obtained, and their characteristics are described in Table 1. This research was approved by the Institutional Ethics Committees of the First Affiliated Hospital of Chongqing Medical University and followed the principles of the Declaration of Helsinki.

Analyses using online databases

The MethHC database tool (http://methhc.mbc.nctu.edu.tw/) was used to analyze the correlation of *IRF8* methylation and gene expression in NSCLC samples compared to normal lung tissue samples. The relationships between IRF8 expression and NSCLC patient survival were analyzed using the Kaplan-Meier plotter data base (http://kmplot.com/analysis/). The threshold search value used for this study was a *p*-value of < 0.05.

DNA extraction and methylation-specific polymerase chain reaction (PCR)

Genomic DNA was extracted following the QIAamp DNA mini kit instructions (Qiagen, Hilden, Germany). DNA were then modified by sodium bisulfite following the protocol of the EZ DNA methylation-gold kit (Zymo Research, Irvine, CA, USA). MSP were performed as described previously [17]. The primers designed to amplify both methylated and unmethylated sequences of *IRF8* are listed in Table 1. Methylation-specific PCR (MSP) was done using AmpliTaq Gold reagents (Zymo Research) with 40 cycles for both methylation and unmethylation-specific primers with annealing temperature of 60°C for the former and 58°C for the latter.

RNA extraction

RNA was extracted from cell lines and tissue samples using TRIzol reagent (Molecular Research Center, Cincinnati, OH, USA). The concentrations of RNA samples were determined by spectrophotometry and samples were stored at -80°C. RNA was reverse transcribed using a Reverse Transcription System (Promega, Madison, WI, USA). Semi-quantitative PCR was carried out using Go-Taq DNA polymerase (Promega) and reaction conditions were as described above. Real-time PCR used ABI SYBR Green on an ABI 7500 real-time PCR detection system (Applied Biosystems, Carlsbad, CA, USA) according to the protocols in the instructions. GAPDH was used as a loading control. Each sample was measured in triplicate. All primers are shown in Table 1.

Demethylation treatment

The A549 and H1299 cell lines were seeded in 100 mm dishes at a density of 1×10^5 cells/ml. After 24 h, the cells were treated with the DNA demethylating reagent 5-Aza-2'-deoxycytidine (Sigma-Aldrich, St. Louis, MO, USA) and histone deacetylase inhibitor trichostatin A (TSA; Cayman Chemical Co, Ann Arbor, MI, USA) as described . Cells were harvested and *IRF8* mRNA was analyzed by RT-PCR.

Plasmid and generation of stable cell lines

The pcDNA3.1(+)-IRF8 plasmid was generated as previously described [18], and the sequences were verified. The full-length IRF8 expressing plasmid was transfected into the H1299 and A549 cell lines using Lipofectamine 2000 (Invitrogen, Carlsbad, CA, USA).To establish stable cell lines, the cells were selected in 200 or 400 μg/mL of G418 for 14 days, and maintained in 100 or 200 μg/mL of G418. IRF8 mRNA and protein over-expression were confirmed by RT-PCR and western blotting, respectively.

Colony-formation assays

The H1299 and A549 cells stably transfected with pcDNA3.1 –IRF8 or empty vector were plated in 6-well plates at a density of 800 cells/well in culture media and G418. After 14–21 days, cells were fixed with 4% paraformaldehyde (PFA) and stained with Crystal Violet solution. Colonies with > 50 cells per colony were counted. All experiments were conducted three times in triplicate.

Cell proliferation assays

Cell proliferation was assessed by the [3-(4, 5-dimethylthiazol-2-yl)-5-(3- carboxymethoxyphenyl)-2-(4-sulfophenyl)-2H-tetrazolium] (MTS) assay [19]. Stable IRF8 expressing and empty vector cells were seeded in 96-well plates (3, 000 cells/well) with 100 μL of medium. Cells were incubated for 24, 48, or 72 h, then 20 μL of MTS solution diluted in 100 μL/well serum-free media was added to each well. Incubation was at 37°C for an additional 2 h. The absorbance was measured at 490 nm using a microplate reader (Multiscan MK3; Thermo Fisher Scientific, Scotts Valley, CA, USA). The experiments were conducted three times.

Cell migration and invasion assays

Cell migration and invasion ability was also measured using Corning Transwell® chambers (8-μm pore size; Corning, NY, USA) and followed the manufacturer's instructions. Cell lines stably expressing pcDNA3.1–IRF8 were used. Twenty-four h after seeding, cells on the lower side of the inserts membrane were counted after staining with 0.1% Crystal Violet. The images were captured in six random fields using a microscope (Leica). All experiments were independently repeated three times. Cells were individually counted by three different persons.

Cell cycle assays

Stably transfected cells were washed in phosphate-buffered saline (PBS) and fixed in 70% ethanol and stained with propidium iodide (PI)/RNase Staining Buffer (BD Biosciences, Franklin Lakes, NJ, USA). Cells were then sorted using a FACSCalibur instrument (BD Biosciences). Data were analyzed by ModFit, version 3.0 software (Verity Software House, Topsham, ME, USA).

Apoptosis assays

Cells transiently transfected with 4 μg pcDNA3.1-IRF8 or empty vector were then stained using Annexin V-FITC/PI staining for apoptosis analyses. Data were analyzed using CellQuest™ Pro (BD Biosciences, San Jose, CA, USA).

Acridine orange/ethidium bromide (AO/EB) fluorescence staining was also used to identify cell apoptosis as previously described [15]. After 48 h transfection, the cells were washed with PBS and stained with AO/EB solution (100 μg/mL, 1:1; Solarbio, Beijing, China), then immediately recorded the images by fluorescence microscopy (Leica CTR4000B; Wetzlar, Germany).

Western blotting

Stably transfected vector or pcDNA3.1-IRF8-transfected cells were washed three times with ice-cold PBS and then protein was extracted [19]. 40μg protein sample was prepared and western blotting was carried out as previously described [19]. The primary antibodies used were as follows: anti-IRF8 (#D20D8; Cell Signaling Technology, Danvers, MA, USA), anti-p21 (#sc-126; Santa Cruz Biotechnology, Santa Cruz, CA, USA), anti-p27 (#sc-393380; Santa Cruz Biotechnology, Santa Cruz, CA, USA), cleaved anti-caspase-3 (#9661; Cell Signaling Technology), cleaved anti-PARP (#9661; Cell Signaling Technology), anti-β-catenin (#2677; Cell Signaling Technology), anti-active-β-catenin (#05-665; Merck Millipore, Billerica, MA, USA), anti-cyclin D1 (#2261; Epitomics, Burlingame, CA), anti-c-Myc (#1472-1; Epitomics, Burlingame, CA), anti-MMP7 (1:1000, #3801; Cell Signaling Technology), anti-BAX (#9942; Cell Signaling Technology), and

with anti-GAPDH (#bsm-51010M; Bioss Antibodies, Woburn, MA,USA) as a loading control. The dilution of primary and secondary antibodies were according to the company's recommendations. The protein bands were detected with the enhanced chemiluminescence kit (Amersham Pharmacia Biotech, Piscataway, NJ, USA)

Dual luciferase reporter assays

TCF/LEF transcriptional activity was determined by luciferase reporter assays.The TCF-responsive luciferase construct pTOPFlash (kindly provided by Professor Tao Qian, Chinese University of Hong Kong, Hong Kong, China), and the FOPFlash reporter containing mutant TCF/LEF binding sites (a gift from Professor Tao Qian) were co-transfected with either pcDNA3.1-IRF8 or empty vector, together with an internal Renilla luciferase reporter control, phRLTK (Promega). Forty-eight h after transfection, luciferase activities were determined using a dual-luciferase reporter assay kit (Promega).

Three-dimensional culture

Stable IRF8 expressing A549 cells and empty vector 3-D cultured cells were cultured following the protocol of Bissell et al. [20]. Matrigel (BD Matrigel™) was seeded in pre-chilled 24-well plates at 120 uL/well. Then, the cells were incubated at 37°C for at least 30 min for the Matrigel to gel. The cells were cultured at a density of 4×10^4 cells/well in culture media containing 10% Matrigel, and were seeded on top of the gel-coated surface. After 24 h, the cells were fixed with 4% PFA and images were captured.

Cisplatin treatment

Cisplatin was purchased from QiLu Pharma (Shan Dong, China).

Stable cell pools expressing IRF8 were treated with cisplatin at concentrations of 0, 2.5, 5, 10, 15, or 20 μg/mL for 12 h, and then collected for MTS analyses.

ChIP-qPCR

The SimpleChIP® Enzymatic Chromatin IP Kit (Cell Signaling Technology) was used for ChIP analyses. Cell isolation, sonication, ChIP analyses, elution, and de-crosslinking of protein complexes by immunoprecipitation were performed according to the manufacturer's instructions. Immunoprecipitated DNA was detected with both real-time PCR and semi-quantitative PCR. The primer sequences are listed in Table 1. The following antibody was used:

Anti-Myc-Tag (#2276 (9B11) mouse monoclonal antibody; Cell Signaling Technology). Fluorescence semi-quantitative PCR was performed using DNA fragments from each immunoprecipitation and from each input sample, and the data were analyzed using percent of input and fold-change.

Immunofluorescence staining

Cells were cultured on coverslips and transfected with IRF8 or empty vector. Forty-eight h after transfection, cells were fixed for 10 min in 4 % PFA, then permeabilized for 4 min in 0.1% Triton X-100 in PBS. Cells were blocked for 1 h with 1% bovine serum albumin in PBS and then incubated with primary antibodies against IRF8 (#sc-6058; Santa Cruz Biotechnology), total-β-catenin (#2677; Cell Signaling Technology), or active-β-catenin (#05-665-AF555; Merck Millipore, Billerica, MA, USA), overnight at 4°C. Nuclei were counterstained with DAPI. Images were captured using a fluorescence microscope (Leica DM IRB, Leica).

Wnt agonist treatment

Stable IRF8 expressing cell lines and empty vector cells were treated with Wnt agonist bml284 agonist at 0.7 μM for 12 h [21]. Protein was then extracted and western blotting was used as described before.

In vivo tumorigenicity

IRF8 stable expressing cells or empty- vector (5×10^6 cells in 0.2ml serum-free medium) were injected subcutaneously into female BALB/c nude mice (4-week-old, five mice/group).Tumour volume (mm^3) was calculated through the following equation: volume=0.5×length×width^2. When the length of tumour reached about 1 cm, the xenograft tumors were removed. The tumor weight was assessed and then tumors were

excised, fixed, dehydrated and embedded in paraffin for immunohistochemistry and HE staining. The animal experiment were authorized by the Committee on Ethical Use of Animals of the Chongqing Medical University.

Statistical analysis

All data are representative of three independent experiments and presented as Mean±SD. SPSS16.0 software was used for Statistical analyses. χ^2 test, were used to compare IRF8 promoter methylation status and clinicopathological parameters. For all tests, p <0.05 was considered statistically significant.

Results

The downregulation of IRF8 mRNA levels correlated with its promotor methylation status in lung cancer

Semi-quantitative RT-PCR was carried out to examine the expression of *IRF8* mRNA in 26 paired human lung cancer tissues and surgical margins. The *IRF8* mRNA level was downregulated in 80.8% (21/26) of primary NSCLC tumor tissues compared with their corresponding adjacent tissues (p < 0.0001, Fig. 1A). We have reported that in most lung cancer cell lines *IRF8* was silenced [2]. We identified *IRF8* as frequently downregulated in NSCLC.

Furthermore, to understand the mechanism underlying the downregulation of *IRF8* in lung cancer, MSP was carried out. As confirmed by MSP, *IRF8* was methylated in 75.9% (41/54) of the tumor tissues while only 24.1% of the *IRF8* was methylated (13/54) in surgical margin tissues (Fig. 1C). Thus, methylation of *IRF8* was a common phenomenon in NSCLC. To further verify the correlation between DNA methylation and the downregulation of *IRF8*, A549 and H1299 cell lines were treated with the demethylating agents, 5-aza-2′-deoxycytidine (5-Aza) and trichostatin A (TSA), resulting in the restored expression of IRF8 (Fig. 1B). Taken together, these data indicated that promoter CpG island hypermethylation of *IRF8* was the underlying mechanism of its downregulation or low expression in NSCLC.

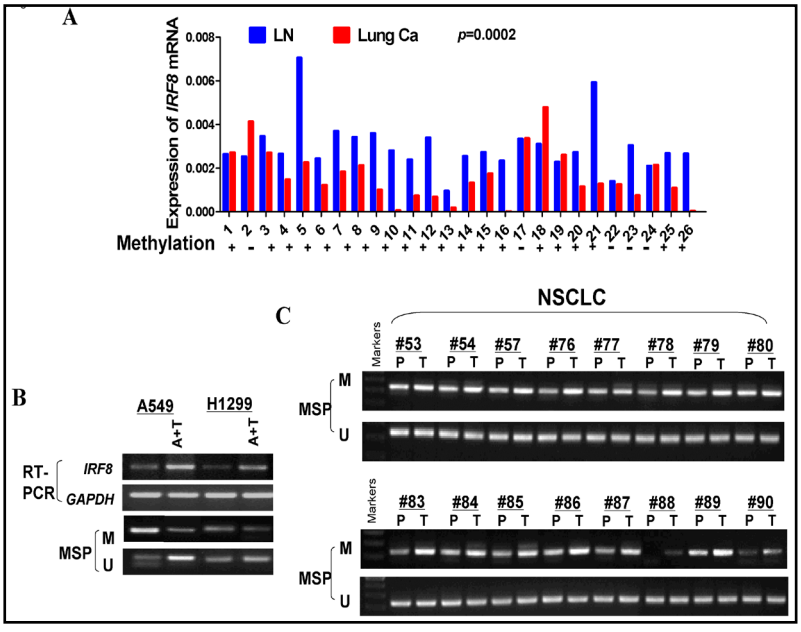

Fig. 1. Downregulation of IRF8 in lung cancer. (A) IRF8 expression in lung cancer tissues and paired surgical margin tissues were evaluated by quantitative RT-PCR analysis. (B) Pharmacological demethylation restored the expression of IRF8 in A549 and H1299 cell lines (A+T), with demethylation of the promoter. M, methylated; U, unmethylated. (C) IRF8 promoter methylation status as determined by MSP in paired lung cancer tissues and tumor adjacent tissues. MSP, methylation-specific PCR.

The expression of IRF8 suppressed cell growth

As previously reported by our group, IRF8 is a tumor suppressor in multiple cancers. In order to test its tumor suppressive functions, we transfected a pcDNA3.1-IRF8 expressing plasmid into the NSCLC cell lines A549 and H1299, which show no or low levels of IRF8. Restoration of IRF8 after stable transfection was verified using RT-PCR and western blotting (Fig. 2A,B). By MTS assays, IRF8 was shown to suppress cell growth in both A549 ($p < 0.01$) and H1299 cell lines ($p < 0.001$) (Fig. 2D). Colony formation assay results further confirmed the results of MTS. The colonies formed by IRF8-expressing cells were significantly less and smaller in both cell lines ($p < 0.001$) when compared to empty vector transfected cells (Fig. 2C).

Restored expression of IRF8-induced cell cycle arrest

To explore the mechanism by which IRF8 inhibits cell growth, we analyzed the effects of IRF8 on cell cycle distribution by using flow cytometry. Stably IRF8 expressing cell lines were used. IRF8 significantly increased cells at the G0/G1 phase (38.19% ± 1.57% versus 67.88% ± 3.34%, $p < 0.001$) in A549 cells, and also in H1299 cells (43.85% ± 1.12% versus 59.66% ± 0.78%, $p < 0.001$) (Fig. 3A,B). Furthermore, western blotting showed that p21 and p27 were upregulated by IRF8 (Fig. 4E). These data suggested that IRF8 induced cell cycle G0/G1 arrest in NSCLC.

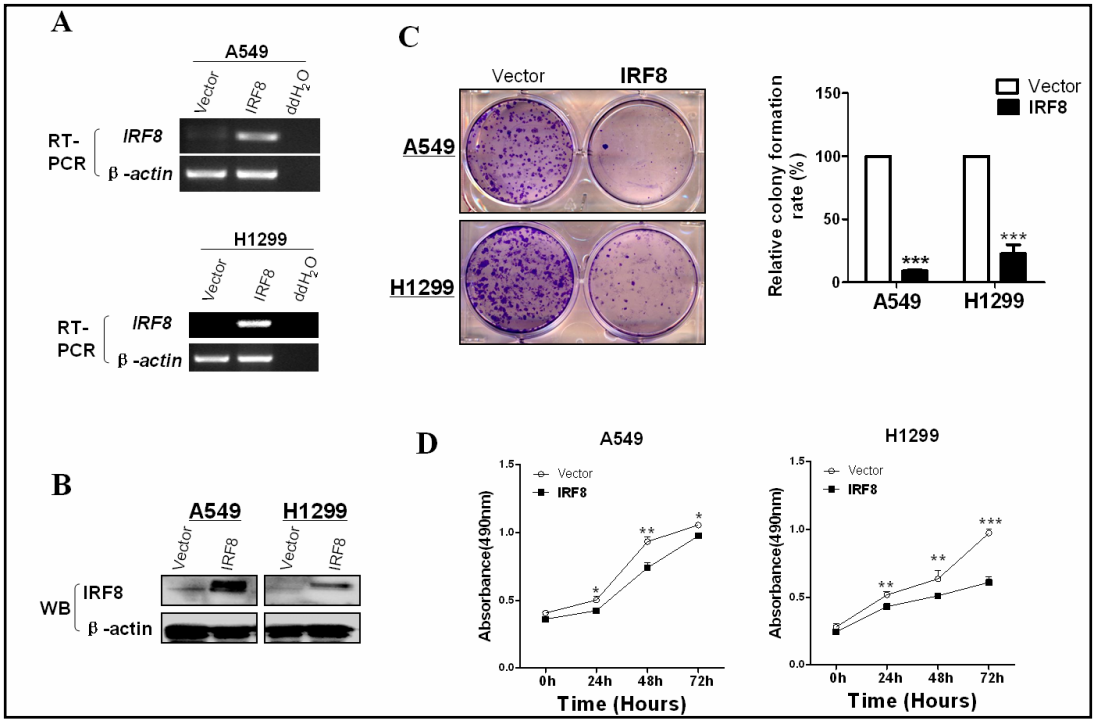

Fig. 2. Ectopic expression of IRF8 suppressed colony formation and cell proliferation in A549 and H1299 cell lines. (A) RT-PCR confirmed the stable re-expression of IRF8 in vector and IRF8-transfected cell lines. (B) Western blot confirmed the stable re-expression of IRF8 in vector and IRF8-transfected cell lines. (C)Ectopic expression of IRF8 inhibited colony formation in A549 and H1299 cell lines. And quantitative analysis of colony formation. The number of colonies in vector-transfected controls were set to 100%. Values are expressed as the mean ± SD from three independent experiments, and the asterisk indicates the statistical significance compared to the controls (***p < 0.001). (D) MTS assay for cell proliferation on vector- and IRF8-transfected stable cell lines. Asterisks indicate a significant level of proliferation compared with controls (**p<0.01, ***p<0.001).

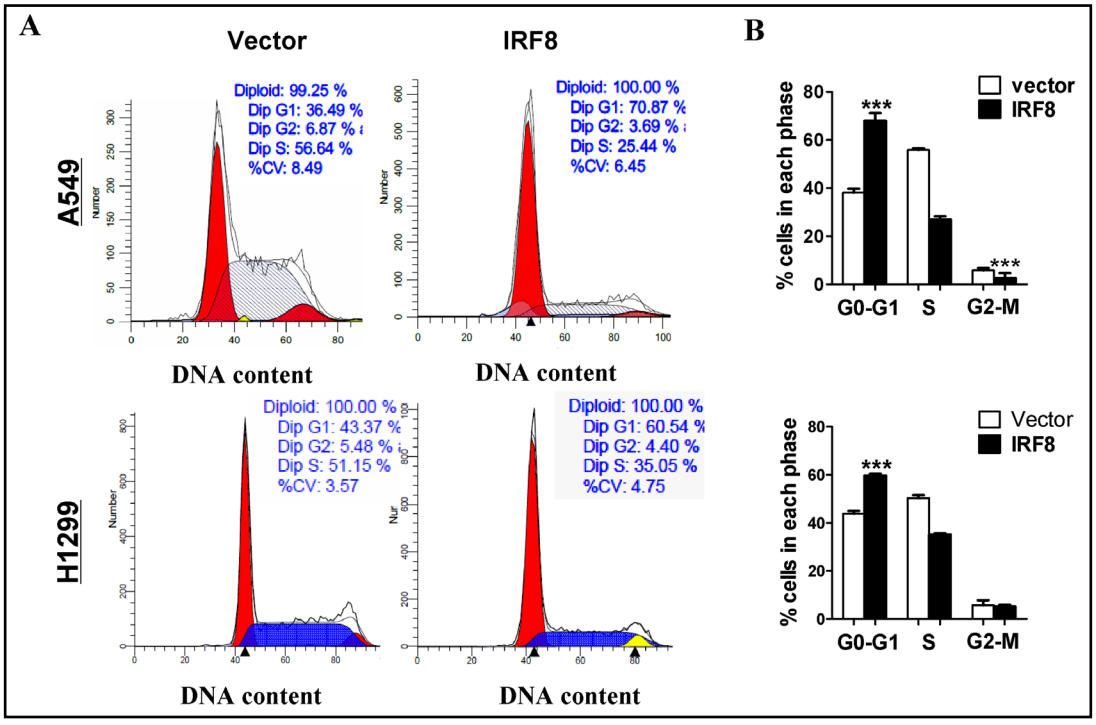

Fig. 3. Restored expression of IRF8-induced cell cycle arrest at the G0/G1 phase in A549 and H1299 cell lines. (A) Representative distribution of A549 and H1299 cell lines both in vector and stable IRF8-transfected cells. (B) The distribution and percentage of cells in G1, S, and G2/M phases of the cell cycle are indicated.

IRF8 induced apoptosis

Flow cytometry analyses showed ectopic expression of IRF8 significantly induced cell apoptosis in A549 (20.65% ± 4.03% vs.30.25% ± 3.17%, $p < 0.001$) and H1299 cells (17.68% ± 1.68% vs. 25.23% ± 0.92%, $p < 0.05$) compared to the empty vector transfected cells (Fig. 4A, B).

To further verify the effects of IRF8-induced apoptosis, AO/EB staining was also used. Early apoptotic cells were stained green with yellow dots, with blebbing cytoplasm, while late apoptotic cells were stained orange with fragmented nuclei. Non-apoptotic cells stained green. AO/EB staining showed both early apoptotic cells and late orange-stained apoptotic cells with fragmented chromatin in the IRF8-expressing group, while the control cells mainly stained green and showed a normal morphology (Fig. 4C,D). Western blotting further verified that the expression of apoptotic markers, Bax, cleaved PARP, and p53 (only observed in A549 cells, while H1299 cells lacked the expression of p53 protein) were increased by IRF8 (Fig. 4E). These data also suggested that IRF8 induced apoptosis in NSCLC cells.

IRF8 repressed NSCLC cell metastasis

To test the effects of IRF8 on NSCLC cell migration and invasive ability, Transwell® migration and invasion assays were performed. As shown in the images, IRF8 significantly suppressed NSCLC cell migration (Fig. 5A)and invasion (Fig. 5B) ability using 10% FBS as a chemoattractant ($p < 0.001$),.

IRF8 induced NSCLC cell morphological changes in three-dimensional culture models

Cell morphological changes in cells stably expressing IRF8 or empty vector were tested in three-dimensional culture systems. A549 cells were established from lung epithelial carcinomas that showed invasive and aggressive phenotypes. As shown in the images, in three-dimensional culture systems, empty vector-expressing A549 cells formed stellate or invasive structures, characterized by spindle-like filopodia and microtubules. Restoration

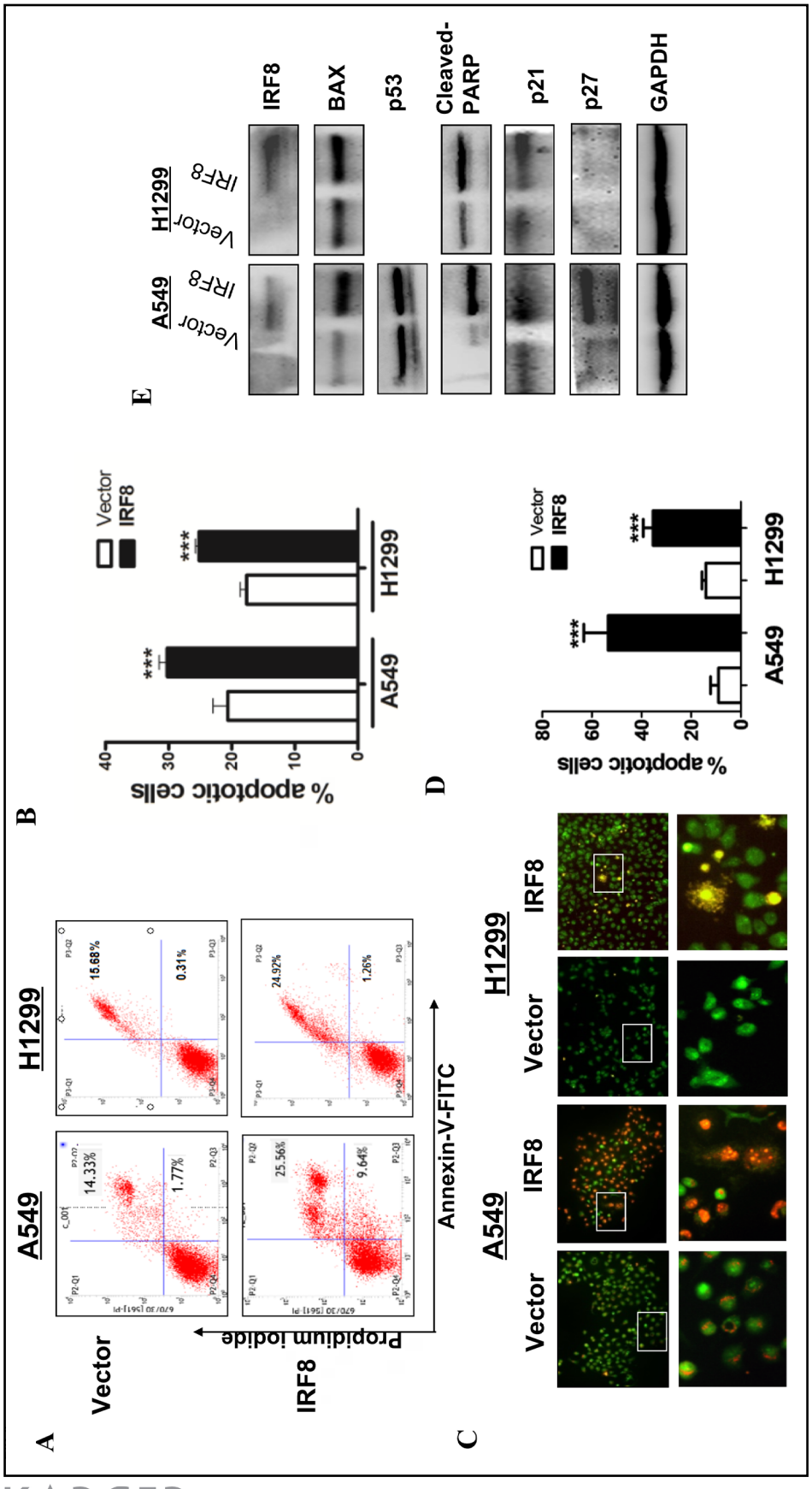

Fig. 4. IRF8 induced cell apoptosis in A549 and H1299 cell lines. (A) Induction of apoptosis detected by flow cytometric analyses with annexin V-FITC and propidium iodide (PI) staining. (B) Quantitative analysis of apoptosis ($p<0.001$). (C) Apoptosis was examined using acridine orange/ethidium bromide (AO/EB) fluorescence staining. The percentage of apoptotic cells is indicated (***$p<0.001$). (D) Quantitative analysis of AO/EB results. (E) Expression levels of Bax, p53, cleaved-PARP, p21, and p27 were evaluated by western blotting of in vector and IRF8-transfected A549 and H1299 cell lines (p53 was deleted in the H1299 cell line).

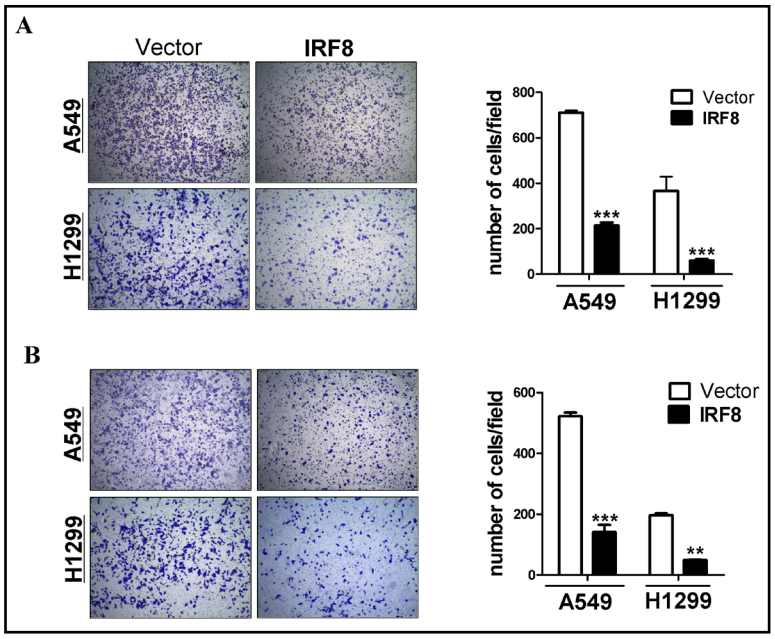

Fig. 5. Ectopic IRF8 expression inhibited cell migration and invasion. (A) Cell migration assay in vector- and IRF8-expressing cell lines by a 24-Transwell® system. Original magnification ×10, p<0.001. (B) Cell invasion assays were carried out in vector- and IRF8-expressing cell lines by a 24-Transwell® system. Original magnification ×10, ***p<0.001,**p<0.01.

of IRF8 changed this invasive shape to irregular spheroids with no or few branching structures and almost no microtubules. This indicated that expression of IRF8 in A549 cells decreased invasive ability by changing the cell shape and reducing cellular interactions (Fig. 6A).

IRF8 enhanced NSCLC cell chemosensitivity to cisplatin

Chemotherapy failure is one of the major causes of cancer recurrence and cancer death of NSCLC. IRF8 was associated with drug resistance in leukemia [15]. In this study, by means of MTS assays, we tested whether the expression of IRF8 enhanced the cisplatin(the most common chemo-reagent used in lung cancer treatment) effects on NSCLC. The results showed that the IC_{50} in the IRF8-expressing cell lines was significantly lower than that of the empty vector-expressing A549 cells (5.28 μg/mL vs. 16.54 μg/mL) and H1299 cells (8.13 μg/mL vs. 12.64 μg/mL) (Fig. 6B), suggesting that IRF8 enhanced chemo-sensitivity to cisplatin in NSCLC.

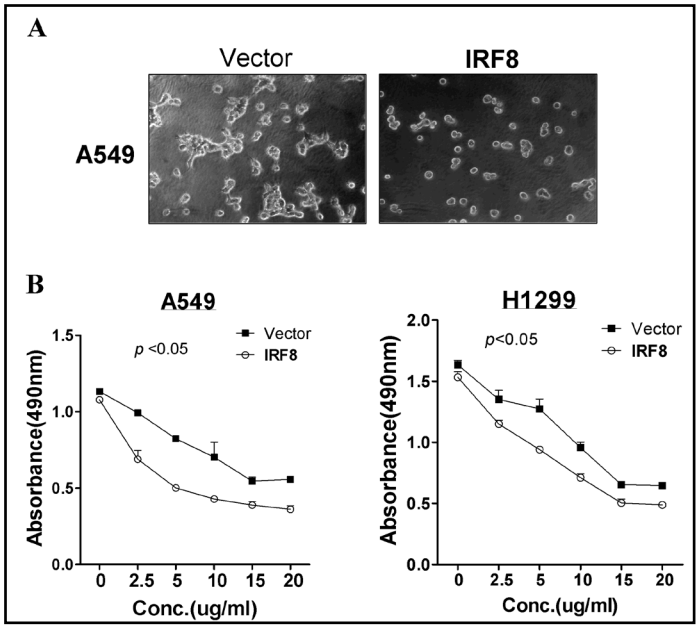

Fig. 6. Ectopic IRF8 expression altered cell morphology and enhanced chemosensitivity to cisplatin. (A) IRF8 induced A549 cell line morphological changes in three-dimensional culture models. Fixed cells were photographed using a phase contrast microscope at 10× magnification. (B) IRF8 enhanced A549 and H1299 cell line chemosensitivity to cisplatin, as determined by the MTS assay (p<0.05).

Identification of LEF/TCF as an IRF8 target gene

To identify IRF8 target genes, we first used the Jaspar data base. The results suggested that IRF8 had a high possibility of binding to the *LEF1* promoter (Table 2). Accordingly, we designed three possible binding sites within the *LEF1* promoter region (Fig. 7A). To test whether IRF8 regulated transcription through the *LEF/TCF* promoter, we performed ChIP-quantitative PCR assays on A549 cells. The IRF8 plasmid used in this study contained a Myc-tag (Fig. 7B). Immunoprecipitation with a Myc-tag antibody resulted in the appearance of a PCR product reflecting the expected *LEF1* promoter fragment. This PCR product spanned the identified IRF8 binding site (Fig. 7C, D). Thus, IRF8 directly bound to the *LEF/TCF* promoter in NSCLC cells, suggesting that *LEF/TCF* could be a IRF8 target gene transcriptionally regulated by IRF8. Furthermore, during the process of β-catenin nuclear translocation and activation, β-catenin formed a complex with LEF/TCF, and was then transported into the nucleus and activated. By binding to the *LEF/TCF* promoter, IRF8 could potentially repress β-catenin activation, and as a result, could be involved in the Wnt/β-catenin pathway.

IRF8 suppressed β-catenin reporter activity.

To further verify that the binding of IRF8 to the *LEF* promoter repressed β-catenin transcriptional activity, RT-PCR and TOP/FOP Flash reporter assays were carried out. The results suggested that IRF8 inhibited *LEF1* and *TCF4* mRNA expression (Fig. 8A). Furthermore, TOPflash/FOPflash reporter assays showed that *IRF8* expression significantly repressed β-catenin transcription in both A549 and H1299 cell lines ($p < 0.001$), with no significant differences in the FOPflash transfected groups (Fig. 8B). These results directly suggested that by binding to the *LEF* promotor, IRF8 downregulated β-catenin mRNA expression and suppressed β-catenin transcription activity.

Table 2. IRF8 binding to the LEF1 promoter predicted by the JASPAR database. 2 putative sites were predicted with these settings. (80%)in sequence named. Chromosome: GRCh 38:4:108170956:-1. The review Nat Rev Genet. 2004 Apr:5(4):276-87 gives a comprehensive overview of transcription binding site prediction

Model ID	Model name	Score	Relative score	Start	End	Strand	Predicted site sequence
MA0652.1	IRF8	5.995	0.821946154455052	345	358	-1	ATGAAAGAGAAAGC
MA0652.1	IRF8	9.257	0.852688638015677	2513	2526	-1	CCGAAGGCGAAACA

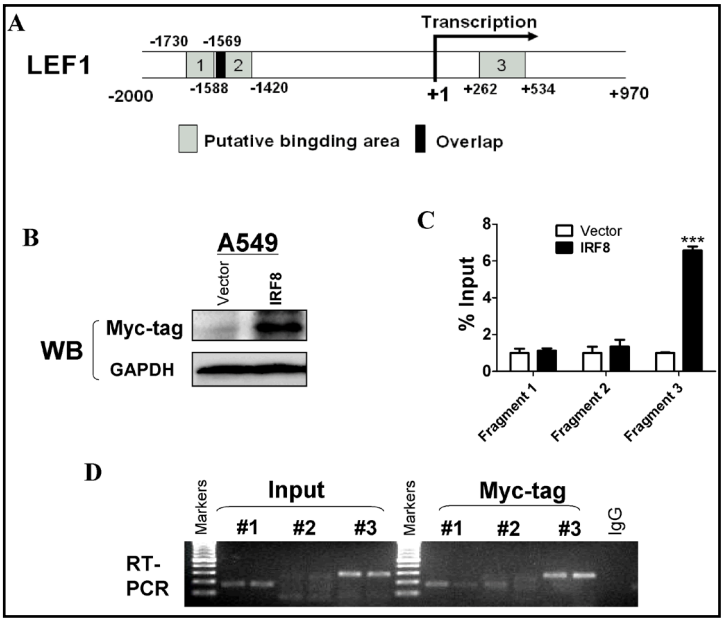

Fig. 7. Identification of LEF/TCF as an IRF8 target gene. (A) Data predicted in the Jaspar database. IRF8 held high possibility of binding to the LEF1 promotor. (B) The designed three possible binding sites in the LEF1 promotor. (C) Western blotting demonstrated the Myc-tag in the IRF8-expressing plasmid. (D) ChIP-quantitative PCR assays on A549 cells. Immunoprecipitation with a Myc-tag antibody resulted in the appearance of a PCR product reflecting the expected LEF1 promoter fragment. (E) Immuno-precipitation products of IRF8 and LEF1 promotor by RT-PCR.

IRF8 downregulated active-β-catenin expression and nuclear translocation as well as its downstream target genes.

Because IRF8 inhibited β-catenin transcription activity, we further tested its effects on β-catenin and downstream gene expression at the protein level, by western blotting. The results suggested that IRF8 repressed TCF4, active-β-catenin protein expression as well as its target genes, C-myc, MMP7, and cyclin D1, while total β-catenin levels remained the same (Fig. 8C).

Because β-catenin activation was affected by IRF8 ectopic expression, β-catenin transport to the nucleus may be essential to its activation. Therefore, we performed immunofluorescence staining to verify the effects of IRF8 on the abundance of nuclear β-catenin, as shown in Fig. 9. After IRF8 overexpression, nuclear β-catenin levels were dramatically decreased, suggesting that by binding to the *LEF* promotor, IRF8 inhibited β-catenin nuclear translocation.

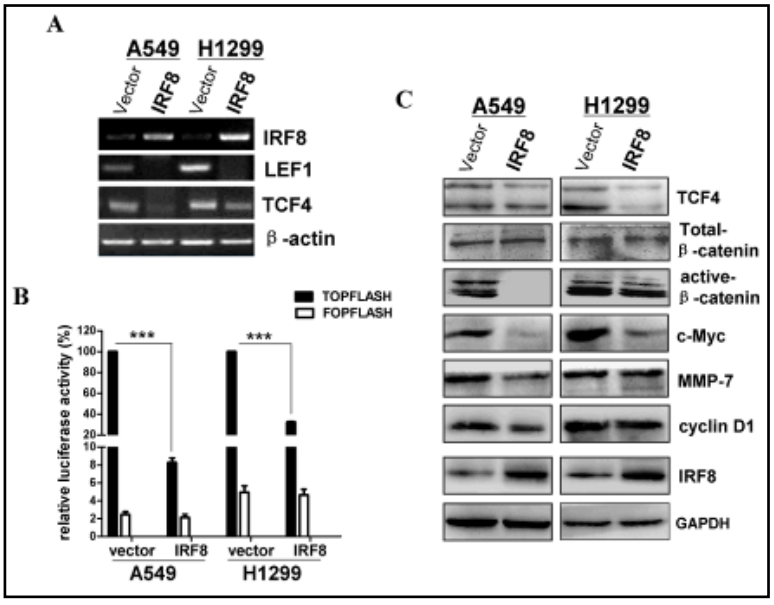

Fig. 8. IRF8 affected β-catenin and its downstream targets in lung cancer cell lines. (A) RT-PCR analysis of LEF1 and TCF4 mRNA levels in vector- and IRF8-expressing cell lines. (B) β-Catenin-TCF/LEF-mediated transcription was determined by the TOPflash luciferase activity assay. FOPflash contained mutant TCF/LEF-1-binding sites and was used as a control. Reporter activities were normalized to a Renilla internal control. (C) IRF8 repressed β-Catenin activation and its downstream targets C-myc, MMP-7, and cyclin D1.

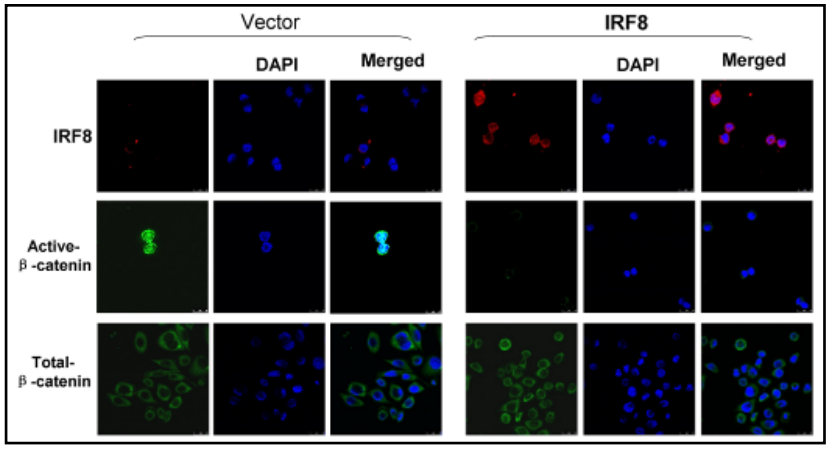

Fig. 9. The effects of IRF8 on the abundance of nuclear β-catenin. Verification by immunofluorescence staining of active β-catenin and total β-catenin in the vector cells and IRF8 expressing cell lines. IRF8 stained red, which was hardly seen in the vector-transfected cells. Active β-catenin stained green in the nucleus and total β-catenin stained green in the cytoplasm;Active β-catenin was decreased by IRF8, while total β-catenin was unaffected.

IRF8 was involved in the Wnt/β-catenin signaling pathway.

The finding that IRF8 regulated different aspects of β-catenin function strongly suggested that these two proteins belonged to the same pathway. To verify this, we stimulated IRF8-expressing and vehicle-expressing cells with Wnt agonists, bml284, and the inducting of β-catenin activation and C-myc and cyclin D1 expressions were measured in empty vector cell lines. The IRF8-expressing cell lines significantly disrupted the stimulating effects of bml284 on the Wnt pathway (Fig. 10A). The results suggested that the binding to the *LEF* promotor regulated β-catenin function, and IRF8 was involved in the Wnt/β-catenin signaling pathway.

IRF8 inhibited xenografted tumor growth in nude mice.

Because IRF8 inhibited lung cancer cell proliferation *in vitro*, we further studied whether IRF8 suppressed lung cancer cell growth in nude mice *in vivo*. Tumor volume were measured every 7 days, and though the growth curve , We can find IRF8 suppressed tumor growth *in vivo* (Fig. 10D).Forty-eight days after injection, tumors were excised from nude mice as shown in (Fig. 10B).The tumor size (Fig. 10B)and mean tumor weight (Fig. 10C) were significantly decreased in the IRF8-overexpressing group vs. the empty vector control group ($p < 0.0001$). Next, by immunohistochemistry, we further validated the Ki-67 levels to determine cell proliferation ability. The expression of HE and ki-67 were significantly downregulated in tumors expressing IRF8 compared with those expressing the empty vector (Fig. 10E), indicating that IRF8 acted as a tumor suppressor in lung cancer *in vivo*.

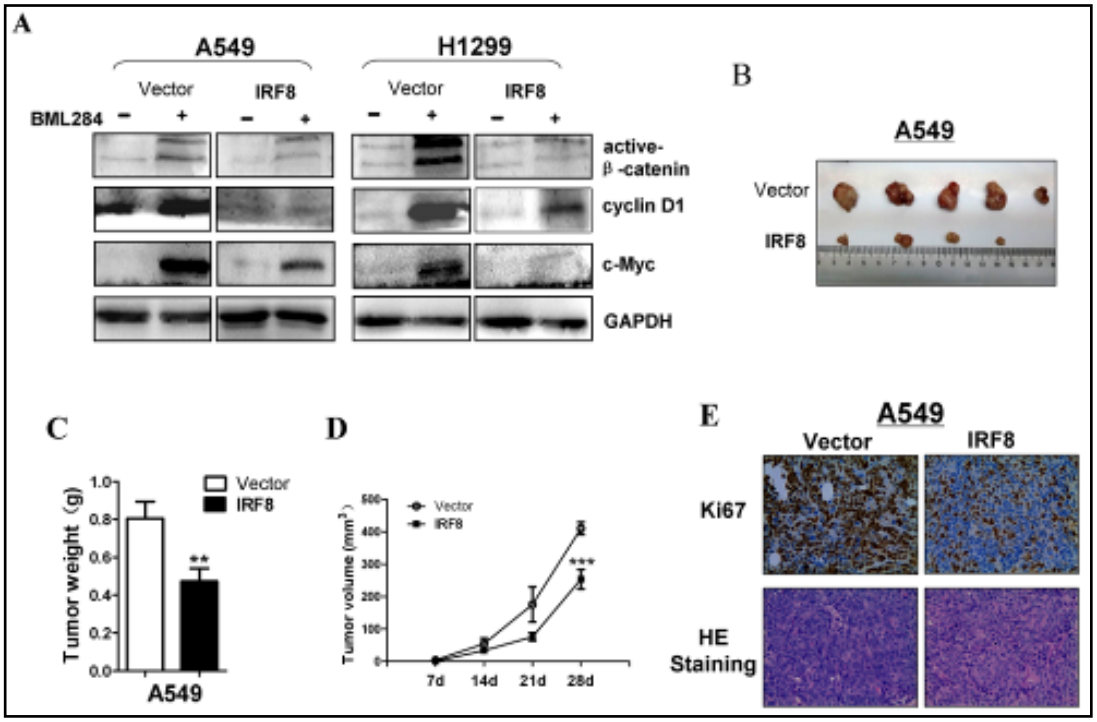

Fig. 10. Effects of IRF8 on the Wnt agonist, bml284,in Wnt pathway activity and IRF8 inhibited xenografted tumor growth in nude mice. (A) Stimulation of IRF8-expressing and vehicle cells with Wnt agonists, bml284, induced β-catenin activation and C-myc and cyclin D1 expression in empty vector cell lines, but this effect was disrupted by IRF8 expression (the developing time was different to Fig. 8C due to some binds were too strong after bml284 treatment). (B) Tumor growth size was significantly decreased in the IRF8 overexpressing group versus the empty vector control group ($p<0.0001$). (C) The mean tumor weight were significantly downregulated in tumors expressing IRF8 compared with vector-expressing cells,($p<0.01$). (D) Tumor growth curve in vivo in IRF8 expressing and vector group.(E) Ki-67 and HE staining by immunohistochemistry, the expression of HE and ki-67 were significantly downregulated in tumors expressing IRF8 compared with vector-expressing cells.

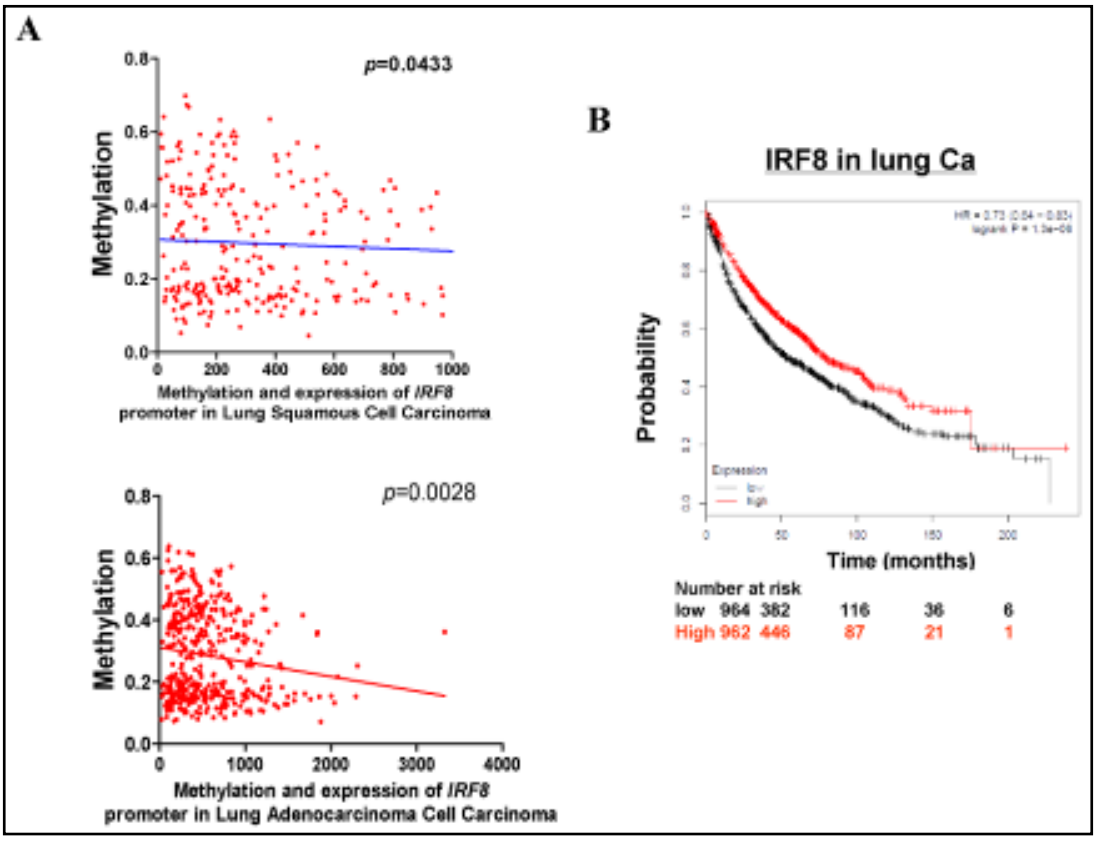

Fig. 11. IRF8 promoter methylation was related to patient clinical pathological features and outcome. (A) The correlation of IRF8 methylation and gene expression in NSCLC samples,and data from The MethHC database tool (http://methhc. mbc. nctu. edu.tw/) . (B) Data in a Kaplan-Meier plotter database (http:// kmplot.com /analysis/) also showed IRF8 expression was related to patient overall survival.

IRF8 promoter methylation was related to patient clinicopathological features and outcomes.

To further verify the correlation of *IRF8* methylation and gene expression in NSCLC samples, the MethHC database tool (http://methhc.mbc.nctu.edu.tw/) was used. The results showed that both in lung squamous cell cancer and adenocarcinoma, *IRF8* promotor methylation was a common event and was closely related to its gene expression (Fig. 11A). Furthermore, we analyzed the relationship between IRF8 expression and NSCLC patient survival using a Kaplan-Meier plotter database (http://kmplot.com/analysis/). The results showed that patients with higher levels of *IRF8* mRNA had significantly increased overall survival compared to those with lower *IRF8* mRNA levels (less than median expression) [hazard ratio (HR) = 0.73; p = 1.3e-06] (Fig. 11B). These results indicated that the IRF8 expression level may serve as an early biomarker to predict the prognosis of lung cancer patients.

We further analyzed the association between *IRF8* promoter methylation and patient clinicopathological features in our lung cancer patient follow-up database. There were 54 patients who were carefully recorded and followed-up. We found that *IRF8* methylation was statistically correlated with important clinical features, such as tumor phase, lymph node metastasis, patient outcome, and tumor histology (χ^2 test, $p < 0.05$), but was not associated with sex, age, tumor size, distant metastasis, and smoking status (Table 3). These results suggested that in lung cancer, IRF8 may be a potential biomarker to predict patient prognosis.

Discussion

Based on previously reported studies by our group, IRF8 was identified as a tumor suppressor in multiple cancers [6]. Its function was verified in renal cancer [22] and breast cancer [23], but its role in the function and mechanisms of NSCLC was unclear. In this study, data revealed that *IRF8* was frequently silenced or downregulated in paired cancer tissues compared to adjacent normal tissues, at the mRNA level. The loss or downregulation of *IRF8* was at least partially associated with its promoter hypermethylation, as confirmed by treatment with the demethylating drugs, 5-Aza and TSA. As shown also by MSP studies, promoter CpG island methylation was the basic regulatory mechanism of *IRF8* inactivation in NSCLC. This result was also confirmed by online data base data analyses. Downregulation of *IRF8* in NSCLC suggested that *IRF8* could be a candidate tumor suppressor gene. Thus, we investigated the tumor suppressive functions of *IRF8* by ectopic expression of IRF8 in human lung cancer cell lines. Restored expression of *IRF8* significantly inhibited cell growth in the NSCLC cell lines, A549 and H1299, induced cell G_0/G1 arrest and apoptosis, and inhibited cell invasion and migration ability. Cell morphological changes are the basic steps in epithelial-mesenchymal changes, and play important roles in cancer invasion. Three-dimensional culture systems were used to show that the re-expression of IRF8 changed the cell morphology from an aggressive to less invasive type. Thus, IRF8 inhibited the cell epithelial-mesenchymal transition in NSCLC. Moreover, because chemoresistance to cisplatin is common in NSCLC, we also observed by use of MTS that IRF8 enhanced chemosensitivity to NSCLC *in vitro*. Collectively, these observations indicated that IRF8 possessed tumor suppressive functions in NSCLC.

Table 3. Clinicopathological features of IRF8 methylation in NSCLC

Clinicopathological features	Number（n=54）	methylated	unmethylated	pvalue
Gender				
Male	43	33（79.1%）	9（20.9%）	
Female	11	7（63.6%）	4（36.4%）	0.420833
Age				
≤50	7	4 (57.1%)	3 (42.9%)	
>50<55	6	2(33.3%)	4 (66.7%)	
55-74	41	34 (82.9%)	7(17.1%)	0.22296
Phase				
Ⅰ	20	12 (63.2%)	8 (36.8%)	
Ⅱ	12	11(84.6%)	1 (15.4%)	
Ⅲ	15	11 (73.3%)	4 (26.7%)	
Ⅳ	7	6 (85.7%)	1(14.3%)	0.00807
Tumour size				
<3.0 cm	28	21(75.0%)	7(25.0%)	
≥3.0 cm≤5.0cm	20	14 (53.6%)	6（46.4%）	
≥5.0cm≤7.0cm	5	4（72.7%）	1（27.3%）	
≥7.0 cm	1	1（100%）	0	0.11091
Lymph node metastasis				
present	28	23（66.7%）	5（33.3%）	
absent	26	17（47.5%）	9（52.5%）	0.034525
Distant Metastasis				
present	7	5（100%）	2	
absent	47	35（52.4%）	12（47.6%）	0.2487
Outcome				
alive	21	14（66.7%）	7(33.3%)	
dead	16	13(81.3%)	3(18.7%)	0.02705
unclear	17			
Smoking status				
smoker	35	26(74.3%)	9(25.7%)	
non-smoker	19	14(73.7%)	5(26.3%)	0.088079
Tumor Histology				
Adenocarcinoma	24	19(79.2%)	5(20.8%)	
SqCa	27	20(74.1%)	7(25.9%)	0.02357
Adeno+SqCa	3			

We next clarified the molecular mechanisms underlying the tumor suppressive functions of IRF8. Apoptosis is a crucial factor in the process of stress induction of tumorigenesis. Yang et al, reported that IRF8 was an essential mediator of apoptosis in nonhemopoietic tumor cells [24] . We also studied the anti-apoptosis function of IRF8. By means of flow cytometry, we showed that IRF8 induced apoptosis of lung cancer cells, and by AO/EB staining we directly showed that apoptotic cells staining yellow and orange were increased by IRF8 overexpression. We further tested apoptotic markers, Bax, PAPR, caspases, and p53, which were upregulated after IRF8 expression. Taken together, we demonstrated the anti-cancer function of IRF8.

Wnt/β-catenin alterations are prominent in human malignancies. In NSCLC, β-catenin and APC mutations are uncommon, but evidence has indicated that Wnt signaling was important in NSCLC cell lines. Available data suggested that Wnt signaling substantially impacted NSCLC tumorigenesis, prognosis, and resistance to therapy, with loss of Wnt signaling inhibitors by promoter hypermethylation appearing to be particularly important in NSCLC. Agents blocking selected specific β-catenin interactions and approaches to

increased expression of downregulated Wnt inhibitors may be of particular interest [7, 25-27] in the future. Scheller et al. identified *Irf8* as a novel Wnt/β-catenin activated target gene that limits myeloid differentiation and proliferation [14]. However, how IRF8 limits the oncogenic processes of the Wnt/β-catenin pathway remains unclear. It was reported that IRF8 regulated β-catenin through PTPN13 [28] and GAS2 [29], but there is none reported direct role of IRF8 in the Wnt pathway. In this study, for the first time, we identified *LEF/TCF* as an IRF8 target gene, by Chip-qPCR, which was correlated with the predicted results from the JASPAR database. Second, TOP/FOP Flash reporter assays and RT-PCR verified that through transcriptionally repressed *LEF/TCF*, IRF8 suppressed β-catenin transcriptional activity. As further confirmed by western blotting, β-catenin activation and its downstream targets were inhibited as a result of the binding between *IRF8* and *LEF/TCF* promotors. In the Wnt/β-catenin pathway, the binding of β-catenin to LEF/TCF resulted in β-catenin translocation from the cytoplasm to the nucleus where it was activated. This is a key step of β-catenin and downstream target activation. Immunofluorescence staining demonstrated ectopic expression of IRF8 inhibited nuclear β-catenin. IRF8 disrupted the agonistic action of the Wnt agonist, bml284, suggesting its involvement in the Wnt pathway. It was reported that IRF8 is a direct target of β-catenin [15]; it can, in turn, block oncogenic β-catenin function. However, how IRF8 represses β-catenin function remains unclear. Our findings revealed that by regulating LEF/TCF, IRF8 inhibited β-catenin and served as an inhibitor of the Wnt signaling pathway. Taken together, our findings and that of other groups revealed a link between IRF8 and β-catenin. Next, we confirmed that IRF8 acted as a tumor suppressor *in vivo* in nude mice. In addition, by MSP, we determined the *IRF8* promotor status and patient clinical signature, and the results suggested IRF8 was correlation with tumor phase, lymph node metastasis, patient outcome, and tumor histology. Data using a Kaplan-Meier plotter database *(*http://kmplot.com /analysis/*)* also showed IRF8 expression was related to patient relapse-free survival. This suggested that IRF8 served as a potential biomarker in NSCLC prognosis.

Conclusion

Taken together, our data demonstrated that IRF8 possessed a tumor suppressive function in NSCLC and directly bound to the *LEF/TCF* promotor. IRF8 repressed β-catenin activity and nuclear translocation, thus acting as a suppressor of the canonical Wnt signaling pathway. Loss of IRF8 as a Wnt signaling inhibitor, by promoter hypermethylation, appears to be particularly important in NSCLC. Blocking specific IRF8/LEF interactions and using approaches to upregulate IRF8 may be of particular interest in lung cancer treatment and prognosis.

Acknowledgements

The authors thank Prof. Qian Tao (Cancer Epigenetics Laboratory, Department of Clinical Oncology, the Chinese University of Hong Kong, Hong Kong, China) for generously providing plasmid primers, cDNA, cell lines and other reagents, technical assistance, and helping with the whole design of the experiment.

This study was supported by Major Projects of International Cooperation and Exchanges, National Natural Science Foundation of China (#31420103915), National Natural Science Foundation of China (#81572769, #81772869), VC special research fund from The Chinese University of Hong Kong, Natural Science Foundation, Yuzhong District Commission of science and technology of Chongqing, China (20170831-18).

Disclosure Statement

The authors report no conflict of interests.

References

1 New M, Keith R: Early Detection and Chemoprevention of Lung Cancer. F1000Res 2018;7:61.
2 Hirsch FR, Merrick DT, Franklin WA: Role of biomarkers for early detection of lung cancer and chemoprevention. Eur Respir J 2002;19:1151-1158.
3 Wiest JS, Franklin WA, Drabkin H, Gemmill R, Sidransky D, Anderson MW: Genetic markers for early detection of lung cancer and outcome measures for response to chemoprevention. J Cell Biochem Suppl 1997;28-29:64-73.
4 Kathuria H, Gesthalter Y, Spira A, Brody JS, Steiling K: Updates and controversies in the rapidly evolving field of lung cancer screening, early detection, and chemoprevention. Cancers (Basel) 2014;6:1157-1179.
5 Roche J, Gemmill RM, Drabkin HA: Epigenetic Regulation of the Epithelial to Mesenchymal Transition in Lung Cancer. Cancers (Basel) 2017;9:1407-1413
6 Lee KY, Geng H, Ng KM, Yu J, van Hasselt A, Cao Y, Zeng YX, Wong AH, Wang X, Ying J, Srivastava G, Lung ML, Wang LD, Kwok TT, Levi BZ, Chan AT, Sung JJ, Tao Q: Epigenetic disruption of interferon-gamma response through silencing the tumor suppressor interferon regulatory factor 8 in nasopharyngeal, esophageal and multiple other carcinomas. Oncogene 2008;27:5267-5276.
7 Stewart DJ, Chang DW, Ye Y, Spitz M, Lu C, Shu X, Wampfler JA, Marks RS, Garces YI, Yang P, Wu X: Wnt signaling pathway pharmacogenetics in non-small cell lung cancer. Pharmacogenomics J 2014;14:509-522.
8 Pacheco-Pinedo EC, Morrisey EE: Wnt and Kras signaling-dark siblings in lung cancer. Oncotarget 2011;2:569-574.
9 Zhang M, Shi J, Huang Y, Lai L: Expression of canonical WNT/beta-CATENIN signaling components in the developing human lung. BMC Dev Biol 2012;12:21.
10 Ying Y, Tao Q: Epigenetic disruption of the WNT/beta-catenin signaling pathway in human cancers. Epigenetics 2009;4:307-312.
11 Behrens J, von Kries JP, Kuhl M, Bruhn L, Wedlich D, Grosschedl R, Birchmeier W: Functional interaction of beta-catenin with the transcription factor LEF-1. Nature 1996;382:638-642.
12 Burchert A, Cai D, Hofbauer LC, Samuelsson MK, Slater EP, Duyster J, Ritter M, Hochhaus A, Muller R, Eilers M, Schmidt M, Neubauer A: Interferon consensus sequence binding protein (ICSBP; IRF-8) antagonizes BCR/ABL and down-regulates bcl-2. Blood 2004;103:3480-3489.
13 Gabriele L, Phung J, Fukumoto J, Segal D, Wang IM, Giannakakou P, Giese NA, Ozato K, Morse HC, 3rd: Regulation of apoptosis in myeloid cells by interferon consensus sequence-binding protein. J Exp Med 1999;190:411-421.
14 Scheller M, Schonheit J, Zimmermann K, Leser U, Rosenbauer F, Leutz A: Cross talk between Wnt/beta-catenin and Irf8 in leukemia progression and drug resistance. J Exp Med 2013;210:2239-2256.
15 Xiang T, Li L, Yin X, Yuan C, Tan C, Su X, Xiong L, Putti TC, Oberst M, Kelly K, Ren G, Tao Q: The ubiquitin peptidase UCHL1 induces G0/G1 cell cycle arrest and apoptosis through stabilizing p53 and is frequently silenced in breast cancer. PLoS One 2012;7:e29783.
16 Wang Y, Li J, Cui Y, Li T, Ng KM, Geng H, Li H, Shu XS, Li H, Liu W, Luo B, Zhang Q, Mok TS, Zheng W, Qiu X, Srivastava G, Yu J, Sung JJ, Chan AT, Ma D, Tao Q, Han W: CMTM3, located at the critical tumor suppressor locus 16q22.1, is silenced by CpG methylation in carcinomas and inhibits tumor cell growth through inducing apoptosis. Cancer Res 2009;69:5194-5201.
17 Zhang L, Zhang Q, Li L, Wang Z, Ying J, Fan Y, He Q, Lv T, Han W, Li J, Yang Y, Xu B, Wang L, Liu Q, Sun Y, Guo Y, Tao Q, Jin J: DLEC1, a 3p tumor suppressor, represses NF-kappaB signaling and is methylated in prostate cancer. J Mol Med (Berl) 2015;93:691-701.
18 Tao Q, Huang H, Geiman TM, Lim CY, Fu L, Qiu GH, Robertson KD: Defective de novo methylation of viral and cellular DNA sequences in ICF syndrome cells. Hum Mol Genet 2002;11:2091-2102.
19 Ying J, Srivastava G, Hsieh WS, Gao Z, Murray P, Liao SK, Ambinder R, Tao Q: The stress-responsive gene GADD45G is a functional tumor suppressor, with its response to environmental stresses frequently disrupted epigenetically in multiple tumors. Clin Cancer Res 2005;11:6442-6449.

20 Vidi PA, Bissell MJ, Lelievre SA: Three-dimensional culture of human breast epithelial cells: the how and the why. Methods Mol Biol 2013;945:193-219.
21 Liu J, Wu X, Mitchell B, Kintner C, Ding S, Schultz PG: A small-molecule agonist of the Wnt signaling pathway. Angew Chem Int Ed Engl 2005;44:1987-1990.
22 Zhang Q, Zhang L, Li L, Wang Z, Ying J, Fan Y, Xu B, Wang L, Liu Q, Chen G, Tao Q, Jin J: Interferon regulatory factor 8 functions as a tumor suppressor in renal cell carcinoma and its promoter methylation is associated with patient poor prognosis. Cancer Lett 2014;354:227-234.
23 Luo X, Xiong X, Shao Q, Xiang T, Li L, Yin X, Li X, Tao Q, Ren G: The tumor suppressor interferon regulatory factor 8 inhibits beta-catenin signaling in breast cancers, but is frequently silenced by promoter methylation. Oncotarget 2017;8:48875-48888.
24 Yang D, Thangaraju M, Browning DD, Dong Z, Korchin B, Lev DC, Ganapathy V, Liu K: IFN regulatory factor 8 mediates apoptosis in nonhemopoietic tumor cells via regulation of Fas expression. J Immunol 2007;179:4775-4782.
25 Zer A, Leighl N: Promising Targets and Current Clinical Trials in Metastatic Non-Squamous NSCLC. Front Oncol 2014;4:329.
26 Skronska-Wasek W, Gosens R, Konigshoff M, Baarsma HA: WNT receptor signalling in lung physiology and pathology. Pharmacol Ther 2018;10.1016/j.pharmthera.2018.02.009.
27 Rapp J, Jaromi L, Kvell K, Miskei G, Pongracz JE: WNT signaling - lung cancer is no exception. Respir Res 2017;18:167.
28 Huang W, Zhu C, Wang H, Horvath E, Eklund EA: The interferon consensus sequence-binding protein (ICSBP/IRF8) represses PTPN13 gene transcription in differentiating myeloid cells. J Biol Chem 2008;283:7921-7935.
29 Huang W, Zhou W, Saberwal G, Konieczna I, Horvath E, Katsoulidis E, Platanias LC, Eklund EA: Interferon consensus sequence binding protein (ICSBP) decreases beta-catenin activity in myeloid cells by repressing GAS2 transcription. Mol Cell Biol 2010;30:4575-4594.